RAPID COMMUNICATIONS

PHYSICAL REVIEW A VOLUME 51, NUMBER 2 FEBRUARY 1995

Angular distribution of high-order harmonics emitted from rare gases at low density

J. Peatross* and D. D. Meyerhofer†

Laboratory for Laser Energetics, University of Rochester, 250 East River Road, Rochester, New York 14623-1299

(Received 22 July 1994)

We have measured the far-field angular distributions of high harmonics (orders 11–41) generated by a 1-μm, 1-ps laser pulse [$(0.3–3)\times 10^{14}$ W/cm^2] in low-density Ar, Kr, and Xe targets ($\leq$1 Torr, 1-mm thick). The far-field harmonic distributions show a narrow central structure surrounded by broad wings that contain approximately 75% of the harmonic energy. Low-density targets and f/70 focusing were used to minimize phase mismatches due to ionization and propagation effects, thereby isolating the single-atom contribution to the response. The wings indicate an intensity-dependent phase of the atomic harmonic emission.

PACS number(s): 42.65.Ky, 32.80.Rm

Laser high-harmonic generation in the noble gases is currently an active area of research. Investigations of these harmonics have so far focused almost exclusively on laser intensity and on propagation effects [1,2]. The extent of harmonic orders has been explored, and photon energies in excess of 100 eV have been observed by a number of groups [2–6]. The generation of high-order harmonics by a laser in an atomic medium can be influenced by several factors: the single-atom response to the laser field, propagation effects (phase mismatches, etc.) due to the wavelength-dependent index of refraction of both the neutral atomic and ionized media, and the geometrical propagation effects inherent in the diffraction associated with a laser focus [1,2,7–9]. In this work we report experiments designed to illuminate the single-atom response to the laser, via a study of the far-field pattern of the emitted harmonics. Our data suggest that the atomic dipole moment responsible for high-order harmonics undergoes phase changes near the peak of the laser pulse and that these are dependent on atomic species. By itself this is not surprising, but our experiments indicate that harmonic angular distributions are a way to study these phase changes.

To investigate the atomic response of the medium, it is essential to characterize the propagation effects as well as possible so that they can be separated out. Our approach to this problem has been to minimize these effects. When harmonic signals emitted from different locations of the interaction region have mismatched phases, the destructive interference not only affects the overall signal but can strongly influence the angular distribution of the emission. This is especially true if the intensity of the driving field is high enough to ionize the medium. This article reports observations of high-order harmonic generation under conditions where propagation effects within the medium are unimportant, even when strong ionization occurs.

In most of the previous experiments, the integrated harmonic emission was measured. The angular (far-field) structure can provide additional information about the harmonic emission process. Recently, we [10,11] and two other groups [6,12] have begun to examine the far-field distribution of the harmonics. Tisch *et al.* [6] have observed the angular distribution of high-order harmonics in He near the plateau cutoff. In these and, to our knowledge, all other experimental observations, the gas target pressure was at least a few torr. Tisch *et al.* found that harmonics that were not near the cutoff showed a central peak and wider, lower-intensity structure. Near the harmonic cutoff, the harmonics were vary narrow. They attribute the wide, low-intensity structure to the phase mismatch associated with the free electrons produced during ionization [6]. Salières *et al.* [12] found that the far-field profile of harmonics generated in ten or more torr showed little far-field structure.

In contrast, we present measurements of the angular distributions of intermediate harmonic orders (11–41) at gas target pressures of less than 1 Torr, where propagation effects from free electrons have a negligible effect on the harmonic far-field profiles [8,9]. These far-field distributions of harmonics of a 1-μm laser were emitted from Ar, Kr, and Xe. The highest observed harmonic in each gas, respectively, was the 41st, 35th, and 29th. All of the harmonics showed a narrow forward peak with a width about one-third that of the laser or less. In addition, many of the harmonics showed broad wings surrounding the peaks with widths about the same as the laser profile. Because of the low gas pressure and large f number used, the structure cannot be due to macroscopic propagation effects in the medium. The wings are attributed to an intensity-dependent phase variation among the dipole moments of the individual target atoms. Such a phase variation gives rise to broad spatial interferences in the scattered light, since the laser intensity varies radially. These results were confirmed by performing a propagation calculation, similar to that of L'Huillier *et al.* [7,8] for our conditions.

The experimental setup is shown in Fig. 1. The harmonics are observed with a transmission-grating spectrometer that provides spectral resolution in one dimension while preserving the angular distribution in the other. The laser used in this experiment has been described in detail elsewhere [13,14]. The wavelength of the light was 1.054 μm, and the pulse duration was monitored by autocorrelation on each shot with a nominal length of 1.4-ps full width at half maximum. Typical laser peak intensities for these experiments ranged from 3×10^{13} to 3×10^{14} W/cm^2. The laser was focused with an

*Also at Department of Physics and Astronomy, University of Rochester, Rochester, NY 14627.

†Also at Department of Mechanical Engineering, University of Rochester, Rochester, NY 14627.

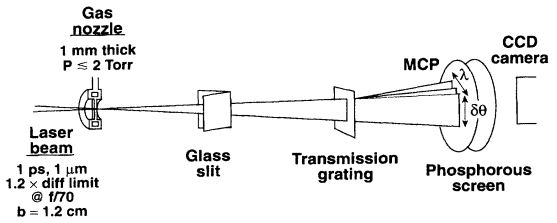

FIG. 1. The experimental setup used in harmonic angular-distribution measurements.

$f/70$ optics, indicating a 13-mm confocal parameter. The diameter of the focal spot was measured to be approximately 1.25 times the diffraction limit.

Near the focus, the laser intersected a thin gas target [15] that provides a low-density, 1-mm gas distribution (cutaway view in Fig. 1). The target consists of two thin metal plates separated by a small gap wherein gas flows. A 0.5-mm hole drilled in the plates allows the laser to pass through without interacting with the metal plates. The density of the gas within the hole remains relatively high, while outside of the hole it disperses quickly. The gas density falls off by more than a factor of 10 at a distance of 1 mm from the hole openings. The target has been characterized experimentally, and the gas distribution is found to be in good agreement with Monte Carlo calculations based on free molecular flow [15].

The harmonics produced in the interaction are collinear with the laser beam. The harmonics must be spectrally resolved without the incident laser pulse damaging the spectrometer. As shown in Fig. 1, a narrow slit (typically 200 μm) was placed 30 cm behind the laser focus, sampling a one-dimensional cut through the center of the laser beam (and the harmonic beams). The slit was made from two pieces of uncoated glass held at an acute angle in order to reduce the intensity on their surfaces. Behind the slit, after the laser light diffracted significantly (not the harmonics), the less-intense light passed through a gold transmission grating with either 1- or 0.2-μm spacing. One or the other grating was sometimes more suitable, depending on the requirements of the measurement. The grating lines were oriented parallel to the slit so that the first-order diffraction of the individual harmonics was resolved after propagating a short distance, where a microchannel plate coupled to a phosphorous screen detected them. Each harmonic appeared as a distinct line that revealed its angular distribution along its length. The images were recorded electronically with a charge-coupled-device (CCD) camera. No signal was observed when the laser was fired through the target with no gas present.

Figure 2 shows an average of 20 CCD camera images of the harmonics as seen on the detector. The harmonics were produced in 0.85 Torr of Xe with a laser intensity of 7×10^{13} W/cm^2. Each harmonic shows a narrow central peak surrounded by broad wings. The 13th harmonic shows the strongest wings that have about the same width as the emerging laser beam ($1/e^2$ radius, 7 mrad). The 0.2-μm grating, which was employed for these shots, attenuated the lower harmonics (lower teens) relative to the higher ones (mid-20's) by about a factor of 5.

In Fig. 2 the central peaks were intentionally saturated on the detector so that the wings could be easily seen. We determined that our microchannel plate (Galileo, model 8081) responds linearly over approximately one order of magnitude. We were able to study the characteristics of the far-field profiles over a much wider range because the gas target employed in these experiments allowed accurate control of the pressure. The harmonic signal was found to follow the quadratic pressure scaling law closely [11].

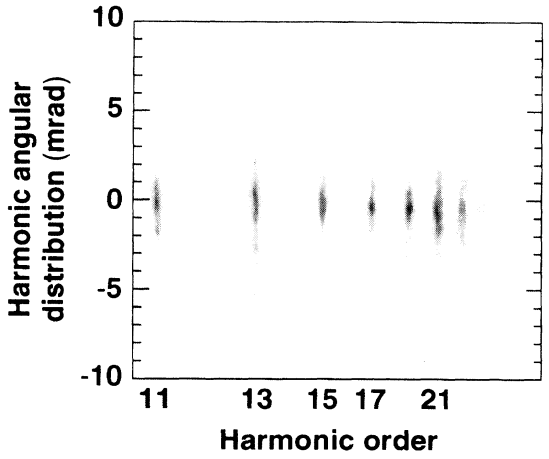

FIG. 2. An average of 20 CCD images of the angular profiles of the 11th–27th harmonics generated in Xe at 7×10 W/cm^2.

Figure 3 shows the angular profiles of the 13th, 15th, and 17th harmonics produced in Ar, Kr, and Xe. Each curve is an average of four shots taken with the 1-μm grating employed in the spectrometer. The peak laser intensity for each gas was at approximately the level where strong ionization begins to occur (2×10^{14}, 1.2×10^{14}, and 8×10^{13} W/cm^2, respectively). Different pressures were used for each gas so that the strength of the signal at the detector was the same. The prominent wings mentioned above can be seen for Xe on the 13th harmonic. The harmonic angular profiles in Kr and Ar have similar behaviors, but the wings in Kr are most pronounced on the 15th harmonic and in Ar on the 17th harmonic. The shift of the pattern with atomic species is evidence that the effect is a manifestation of atomic physics and not simply an artifact of propagation in the medium. The harmonic with the strongest wings for each gas has an energy close to the ionization potential (one plus a fraction of a harmonic above). Owing to the much larger cone angle, the wings typically have about three times the energy associated with the central peaks.

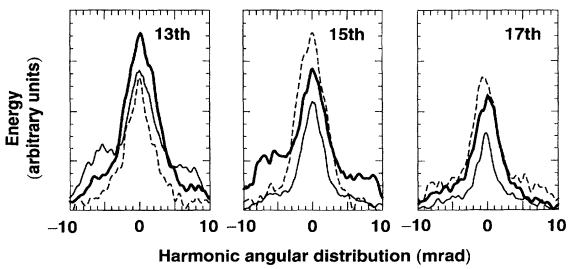

FIG. 3. The 13th, 15th, and 17th harmonics of Ar (dashed), Kr (thin), and Xe (thick). The peak laser intensities were 2.1×10^{14}, 1.2×10^{14}, and 8×10^{13} W/cm^2, respectively.

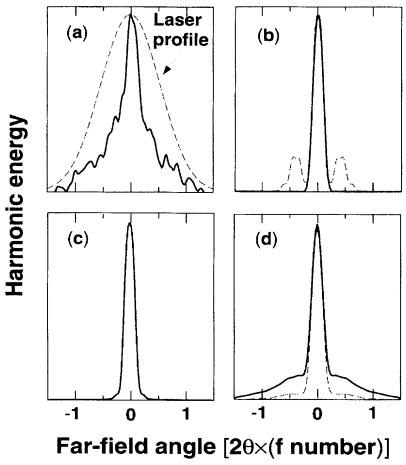

FIG. 4. (a) The measured far-field profile of the 13th harmonic produced in 0.3 Torr of Xe. (b) The calculated far-field profiles of the 13th harmonic for target thicknesses $l=b/13$ (solid) and $l=b$ (dotted). Harmonic production is assumed to be proportional to the laser intensity squared. (c) A calculation similar to the solid curve in (b) but with the effects of ionization at 0.3 Torr included. (d) The far-field pattern of the 13th harmonic calculated from an anharmonic-oscillator model (solid). The dotted curve is calculated in the same way except the intensity-dependent phase is removed.

The fact that the harmonic far-field profiles have widths comparable to the laser's profile, implies that either the harmonic generation is localized within the interaction region to an area q^2 times smaller than the laser beam where q is the harmonic order, or there is a strong phase variation of the harmonic wave front as it exits the medium. The scenario of a very small interaction region can be dismissed because it implies extreme sensitivity of the overall harmonic production to the laser intensity (proportional to intensity to the q^2 power) that is certainly not the case in the regime where we are operating (the region of the harmonic plateau where many harmonic orders are produced with approximately the same efficiency). The alternative, a phase variation in the harmonic beam wave front, can arise from propagation effects within the atomic medium or from an intensity-dependent phase in the production at the atomic level due to the radial laser intensity variation. Because we have minimized propagation effects within the medium, we can conclude unambiguously that the broad wings in our harmonic far-field patterns cannot be due to macroscopic propagation effects and are probably the result of intensity-dependent phase variations at the atomic level.

Figure 4(a) shows the angular distribution of the 13th harmonic generated in 0.3 Torr of xenon with a laser intensity of 7×10^{13} W/cm^2. The curve was obtained from an average of 20 shots, and detector saturation was avoided. The angle is expressed in terms of $2\theta\times(f$ number) so that the $1/e^2$ intensity points of the laser profile occur at ±1. For comparison, Figs. 4(b)–4(d) show harmonic far-field patterns calculated using the full three-dimensional phase-matching integral [1] (including the temporal evolution) for a variety of conditions, as will be explained. All of the calculated curves have been convolved with our detector angular resolution of 1 mrad.

In the intensity range of the harmonic plateau, harmonic production increases only gradually with the laser intensity. Figure 4(b) shows two far-field patterns, calculated assuming that harmonic production is proportional to I^p $(p=2)$ and that the phase of the harmonic when created is q times the local phase of the laser regardless of intensity $(q=13)$. Similar assumptions were used by L'Huillier to show geometric effects in the propagation of harmonics within the atomic medium [1,16]. The solid line is calculated assuming a uniform gas target thickness of $l=b/13$, where b is the laser confocal parameter (our experimental condition), and the dotted line is calculated using $l=b$. In both calculations, the target is centered at the laser focus. The curves have been normalized to the same height. For $b=1/3$, the far-field distribution is virtually the same as if it were calculated from atoms lying within a single plane at the focus, but for $l=b$, the distribution shows that geometric propagation effects can play an important role for a thicker medium. The conclusions are insensitive to the choice of p, up to and including $p=2$.

Figure 4(c) shows a calculation similar to that of the solid line in Fig. 4(b), but the temporal and spatial effects of ionization of the atomic medium are included. The parameters for this calculation are $q=13$, $p=2$, $l=b/13=1$ mm, and $P=0.3$ Torr (our experimental conditions). The ionization rate is taken to be proportional to I^{11} (lowest-order perturbation theory for Xe), and the peak intensity was chosen to be twice the ionization saturation intensity to ensure strong ionization. The result, which is not sensitive to the details of the ionization model, shows that ionization cannot explain the broad wings seen in our data. The small bumps to either side of the central peak are the result of atomic depletion in the interaction region and not the result of phase mismatch due to free electrons. This is because the phase mismatch over 1 mm due to free electrons at 0.3 Torr for the 13th harmonic is 0.1π. In contrast, the phase mismatch due to free electrons at 3 Torr for the 91st harmonic is 3π [6].

Figure 4(d) shows the far-field profile of the 13th harmonic calculated using a classical anharmonic oscillator model $[\ddot{x}+\Gamma\dot{x}+\omega_0^2x=(eE/m_e)\cos\omega_L t-\beta x^3]$ to describe the motion of the bound electrons. The parameters were chosen to simulate xenon by choosing ω_0 to be the atomic binding potential and by choosing β to match a measurement of the third-harmonic emission. Their values are 12.1 eV and 4×10^{-35} (s Å)$^{-2}$, respectively. The solid line in Fig. 4(d) is calculated by including the phase of the harmonic as described by the equation, and the dotted line is calculated from the absolute value of the response so that the phase of the harmonic when created is simply q times the local phase of the laser. Both curves were calculated with $l=b/13$, and the response of the anharmonic-oscillator model to the driving field was included adiabatically. The large difference in the wings of the two cases shows that intensity-dependent phase effects play an important role.

While the anharmonic oscillator presented above is not intended to model a real atom very closely, it is given as an example to show the behavior characteristics of nonlinear systems. A strong intensity-dependent phase variation is a feature common to many high-harmonic-generation models [1,3,5,16–18] and the anharmonic oscillation is qualitatively similar to these models. These phase variations play an im-

portant role in determining the spatial characteristics and coherence of high harmonics emitted from a laser focus.

In summary, the most important finding of this work is the occurrence of broad wings that appear in the far-field pattern of nearly every high harmonic. Because other possible origins for these wings can be discounted for our conditions, we conclude that the phase of the dipole response has a strong laser-intensity dependence. Since the laser intensity varies radially in the interaction region, this intensity dependence implies a radial variation for phase of the dipole emission. Such phase variations can cause the harmonic light to interfere in the far field, leading to broad wings observed. A strong intensity-dependent phase of the atomic dipole response is a feature common to many high-harmonic generation models.

The authors wish to acknowledge useful discussions with B. Buerke, J. H. Eberly, M. H. R. Hutchinson, P. L. Knight, K. Kulander, A. L'Huillier, and R. A. Smith. This work is supported by the National Science Foundation under Contract No. PHY-9200542. Additional support was provided by the U.S. Department of Energy, Office of Inertial Confinement Fusion, under Cooperative Agreement No. DE-FC03-92SF19460, and the University of Rochester.

[1] Ph. Balcou and A. L'Huillier, Phys. Rev. A **47**, 1447 (1993).

[2] A. L'Huillier and Ph. Balcou, Phys. Rev. Lett. **70**, 774 (1993).

[3] C.-G. Wahlström, J. Larsson, A. Persson, T. Starczewski, S. Svanberk, P. Salières, Ph. Balcou, and A. L'Huillier, Phys. Rev. A **48**, 4709 (1993).

[4] N. Sarukura, K. Hata, T. Adachi, R. Nodomi, M. Watanabe, and S. Watanabe, Phys. Rev. A **43**, 1669 (1991).

[5] J. J. Macklin, J. D. Kmetec, and C. L. Gordon III, Phys. Rev. Lett. **70**, 766 (1993).

[6] J. W. G. Tisch, R. A. Smith, J. E. Muffet, M. Ciarrocca, J. P. Marangos, and M. H. R. Hutchinson, Phys. Rev. A **49**, R28 (1994).

[7] A. L'Huillier, K. J. Schafer, and K. C. Kulander, Phys. Rev. Lett. **66**, 2200 (1991).

[8] A. L'Huillier, K. J. Schafer, and K. C. Kulander, J. Phys. B **24**, 3315 (1991).

[9] A. L'Huillier, P. Balcou, and L. A. Lompré, Phys. Rev. Lett. **68**, 166 (1992).

[10] S. Augst, D. D. Meyerhofer, J. Peatross, and C. I. Moore, in *Proceedings of the Topical Meeting on Short-Wavelength Coherent Radiation: Generation and Application*, edited by P. Bucksbaum and N. M. Ceglio (Optical Society of America, Monterey, CA, 1991), Vol. II, pp. 23–27.

[11] D. D. Meyerhofer and J. Peatross, in *Super-Intense Laser-Atom Physics*, edited by B. Piraux, A. L'Huillier, and K. Rzazewski (Plenum, New York, 1993), pp. 19–29.

[12] P. Salières, T. Ditmire, K. S. Budil, M. D. Perry, and A. L'Huillier, J. Phys. B **27**, L217 (1994).

[13] P. Maine, D. Strickland, P. Bado, M. Pessot, and G. Mourou, IEEE J. Quantum Electron. **QE-24**, 398 (1988).

[14] Y.-H. Chuang, D. D. Meyerhofer, S. Augst, H. Chen, J. Peatross, and S. Uchida, J. Opt. Soc. Am. B **8**, 1226 (1991).

[15] J. Peatross and D. D. Meyerhofer, Rev. Sci. Instrum. **64**, 3066 (1993).

[16] A. L'Huillier, P. Balcou, S. Candel, K. J. Schafer, and K. C. Kulander, Phys. Rev. A **46**, 2778 (1992).

[17] L. Plaja and L. Roso-Franco, J. Opt. Soc. Am. B **9**, 2210 (1992).

[18] K. C. Kulander, K. J. Schafer, and J. L. Krause, in *Super-Intense Laser-Atom Physics III*, edited by B. Piraux (NATO, Han-sur-Lesse, Belgium, 1993).

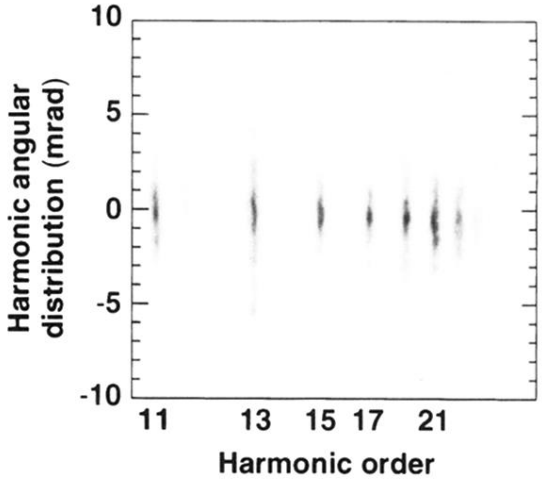

FIG. 2. An average of 20 CCD images of the angular profiles of the 11th–27th harmonics generated in Xe at 7×10 W/cm^2.